Available online at www.sciencedirect.com

ScienceDirect

journal homepage: www.elsevier.com/locate/he

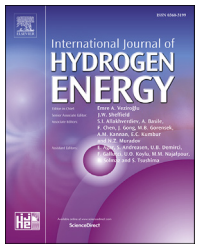

# How the BoP configuration affects the performance in an air-cooled polymer electrolyte fuel cell. Keys to design the best configuration

*A. de las Heras*[*], *F.J. Vivas*, *F. Segura*, *J.M. Andújar*

*Grupo de Investigación de Control y Robótica TEP-192, Departamento de Ingeniería Electrónica, de Sistemas Informáticos y Automática, Escuela Técnica Superior de Ingeniería, Universidad de Huelva, Carretera Huelva – Palos de la Frontera, 21819, La Rábida – Palos de la Frontera, Huelva, Spain*

ARTICLE INFO

*Article history:*
Received 19 July 2016
Received in revised form
28 October 2016
Accepted 7 November 2016
Available online 29 November 2016

*Keywords:*
Air cooled polymer electrolyte fuel cell
BoP configurations
Fuel subsystem design
Experimental study

ABSTRACT

Air Cooled Polymer Electrolyte fuel cells (AC-PEFC) are recently receiving especial attention because they offer the possibility to integrate the oxidant and cooling subsystems in just one. This feature reduces not only the fuel cell weight, volume and cost but also the control complexity. In these fuel cells, the Oxidant/Cooling subsystem along with three others (*Fuel*, *Electrical* and *Control*) make up the Balance of Plant (BoP), which together with the stack comprise the full fuel cell. It is common to find works focused on analysing the influence of the Oxidant/Cooling subsystem on the fuel cell. Nevertheless, studies in which the Fuel subsystem (it is responsible for providing the hydrogen for its reduction–oxidation reaction with oxygen to form water) is investigated are hard to find on the scientific literature. It seems like the Fuel subsystem configuration would not have influence over the whole system performance. Contrary to what one might think, and in basis on experimental results, this paper shows how the fuel cell performance is conditioned by the Fuel subsystem configuration. The aim of this paper is to present a comprehensive experimental study of an AC-PEFC paying particular attention, so unexplored so far, to Fuel subsystem configuration, giving the keys for the most suitable BoP configuration which guarantees the best performance, with the easiest BoP design and the lowest complexity.



## Introduction

As it is widely known, Polymer Electrolyte Fuel Cell (PEFC) is a promising technology due to its high power density, low operating temperature, low pollution level, quiet operation, lower corrosion, simplification of stack design and relatively quick start-up and shut-down [1–3]. Although in the past decades there has been a huge progress in the PEFC field, researchers still continue developing their researches in areas related to new cell designs for better performance, cost reduction, or optimized cold-start characteristics [4]. One of the reason of this continuous research works is because PEFCs are suitable for a wide range of applications, including portable, stationary and automotive power delivery [5–10] and they are having more and more importance in backup systems for emergency situations (e.g. earthquakes, terrorist attacks).

* *Corresponding author.*
E-mail address: ainhoa.delasherasjimenez@gmail.com (A. de las Heras).
http://dx.doi.org/10.1016/j.ijhydene.2016.11.051

**Nomenclature**

| | |
|---|---|
| AC | Air Cooled |
| BoP | Balance of Plant |
| BPP | Bipolar Plates |
| DEA | Dead-End Anode |
| DMFC | Direct Methanol Fuel Cell |
| FC | Fuel Cell |
| FTA | Flow-Through Anode |
| GDLs | Gas Diffusion Layers |
| MEA | Membrane Electrode Assembly |
| PE | Polymer Electrolyte |
| PEFC | Polymer Electrolyte Fuel Cell |
| $P_{H2}$ | Hydrogen Pressure |
| λ | Stoichiometric rate |

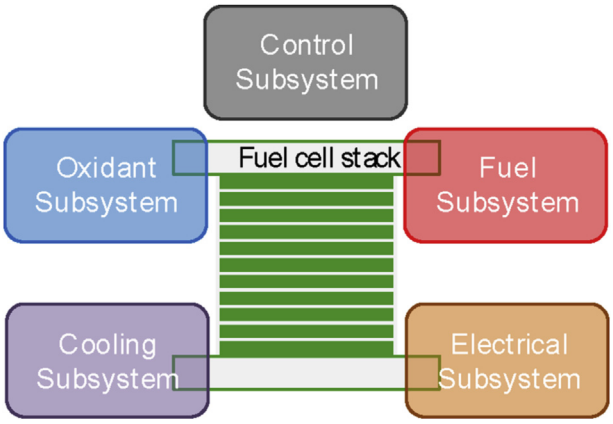


**Fig. 2 – Scheme of a PEFC fuel cell integrated by the stack + BoP (Oxidant, Fuel, Cooling, Electrical and Control subsystems).**

A typical PEFC is formed by six main parts (Fig. 1) from the outermost to the innermost: End Plates, Current Collectors, Bipolar Plates (BPP), Gaskets, Gas Diffusion Layers (GDLs) and Membrane Electrode Assembly (MEA) [11]. For the design of a PEFC from the stack (built by assembling single cells with similar structure to that shown in Fig. 1), it is necessary to incorporate additional subsystems. Generally these can be classified in five groups: *Oxidant*, *Fuel*, *Cooling*, *Electrical* and *Control*, Fig. 2. All of them make up the Balance of Plant (BoP) and they handle the PEFC works properly [12,13]. The role of these subsystems is to supply reactants (oxygen and hydrogen at the appropriate flow and pressure for electrochemical reaction), remove the heat generated in the stack and maintain it at the temperature recommended by the manufacturer, eliminate the water produced, connect the stack to electric load and process information from sensors to control the actuators [14,15].

Previous efforts for the development of PEFC have demonstrated that a reliable design of the BoP is essential for the fuel cell stack operation as it determines the full fuel cell performance. In the BoP design, it is important to optimize the different subsystems, as well as example an oversized BoP configuration results in an increase in parasitic loss, system volume, weight and noise level [16].

Regarding the scheme of Fig. 2, the authors of this study have used an AC-PEFC stack, which integrate Oxidant and Cooling subsystems into one single. This allows that there are no liquid in the Cooling subsystem, thus facilitating and simplifying the BoP integration because they do not need pipes, valves, pumps and heat exchangers, contributing to reduce weight, volume and cost. Another feature of the stack used in this work is that it does not require high inlet hydrogen pressure; indeed, it can operate at pressures close to ambient. This second feature provides security because it is not necessary to work with high hydrogen supply pressure and less stringent requirements in the hydrogen transfer circuit (connections, pipelines, etc.).

Several authors have developed different BoP configurations [15,17–26], and in all these case authors justify the chosen configuration in basis on the conditions required by their systems.

In this sense, there are not too many works in which different configurations are analysed, discussing their advantages and disadvantages. Then Youngseung Na et al. [27]

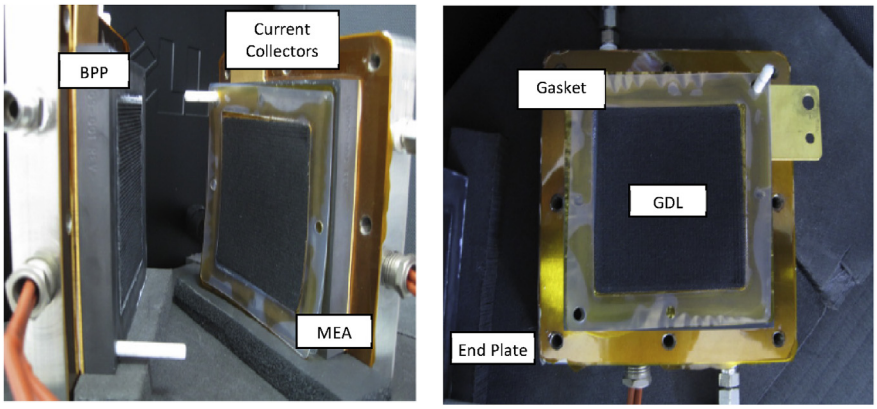


**Fig. 1 – Single fuel cell with a 50 $cm^2$ active area from Teledyne™, with three-channel parallel serpentine flow fields (channels of 0.76 mm wide and deep). Graphite bipolar plate's layout is cross-flow, with horizontal channels in both anode and cathode.**

propose a new experimental technique to improve the performance and stability of the DMFC system under air-blowing conditions, and Kim et al. [28] show two types of Oxidant subsystem (a gas recirculation subsystem with and without a recycle blower). On the other hand, Hinaje et al. [29] evidence the behaviour of a fuel cell system as a current source, in which the current is directly controlled by the hydrogen flow rate. Rodatz et al. [30] show an exhaustive evaluation among the five most important types of the fuel subsystems. Going deeper in this way, Chen et al. [31] summarise all these Fuel subsystem configurations in two groups: Dead-End Anode (DEA) and Flow-Through Anode (FTA) operation mode. In any case, independently of the number of groups done all authors agree with the idea that a DEA Fuel subsystem configuration requires fewer auxiliary components compared to traditional FTA, Fig. 3.

The FTA operation with hydrogen flow control depends on a recirculation loop to maintain a high hydrogen utilization and enhanced convective transport. So this configuration requires additional equipment such as an ejector/blower, a water separator/demister and an anode humidifier. These components add weight, volume, and cost to the system.

Regarding DEA operation, it is possible to adjust the hydrogen inlet stoichiometry to one by regulating the inlet pressure (so it would not be needed the hydrogen recirculation) and the anode channel pressure would remain constant. That is, DEA operation depends on upstream pressure regulation instead of the hydrogen mass flow control. Chen et al. [31] try to control the hydrogen inlet pressure by scheduling the purge interval. The final goal of that work was to improve the output power at time that the hydrogen losses are reduced. Simulation results shown the fuel cell efficiency improvement.

Now, giving a further step we proposes six different configurations for the Fuel subsystem in DEA operation. The basic devices which take part in the hydrogen line are a mass flow meter, a pressure sensor and a purge valve. Around these devices, we will put a proportional control valve and experimental results allow us to corroborate some proposals presented previously. Then, we see for example suggestions as the hydrogen mass flow control is not suitable for the DEA operation. Another key point is the way to regulate the hydrogen inlet pressure (and consequently to adjust the hydrogen inlet stoichiometry), which is usually carried out by means the purge interval schedule. However there may be other alternatives (especially when it comes a stack with low inlet pressure). From these we can configure a half-dozen proposals and we can draw some keys to select the most suitable to optimize the AC-PEFC operation.

This paper is organized as follow. AC-PEFC characterization is done in Section II, explaining its main features as well as giving its experimental polarization and power curves. Section III describes the different BoP configurations implemented, showing each diagram and pointing out the particularities of each one. Next, experimental results obtained from each configuration as well as some discussions about

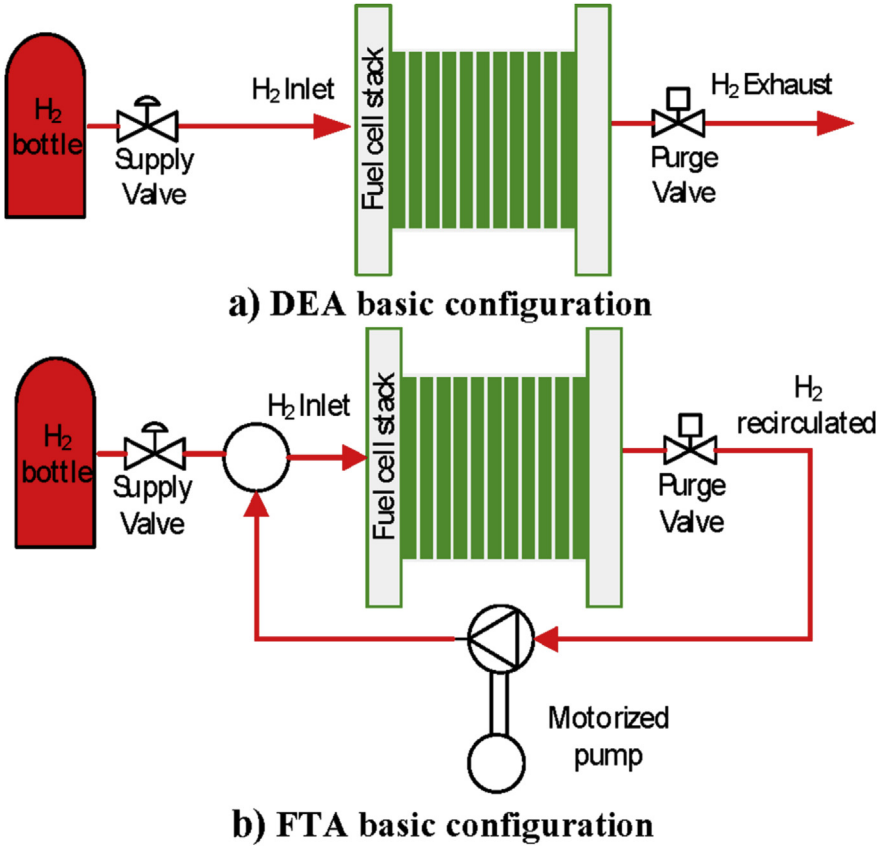


**Fig. 3 – Scheme of DEA versus FTA Fuel subsystem configurations.**

them are summarised in Section IV and V respectively. Finally, Section VI draws the main conclusions derived from the experimental study.

## System characterization

The fuel cell under study is based on the FCgen-1200ACS stack model from Ballard®. This stack is characterised by it is air-cooled and it does not need external air humidification. The operation mode is dead-end using dry hydrogen without humidification. The inlet hydrogen pressure can vary from 1.16 to 1.56 bars. The stack is constituted by 80 cells and, according to manufacturer's data, it can reach up to 3.4 kW [32].

This stack has been used to build a AC-PEFC (Fig. 4) where the (BoP) has been developed according to [17]. The AC-PEFC shown in Fig. 4 has been developed by authors and constitutes an excellent test bench to carry out all kinds of tests on a real system [17].

The configuration of our Oxidant/Cooling subsystem is very simple and effective, consists of an adjustable flow fan (model EbmPapst™ DV6224TDA) and a stack temperature sensor (Ts) included in the own stack (see Fig. 4a and b). Following Fig. 4a, at the fuel input the Fuel subsystem is made up of the hydrogen storage bottle, and a manual pressure regulator to reduce the high pressure from the bottle to pressure range recommended by the stack manufacturer. Additionally, a mass flow meter to measure the hydrogen

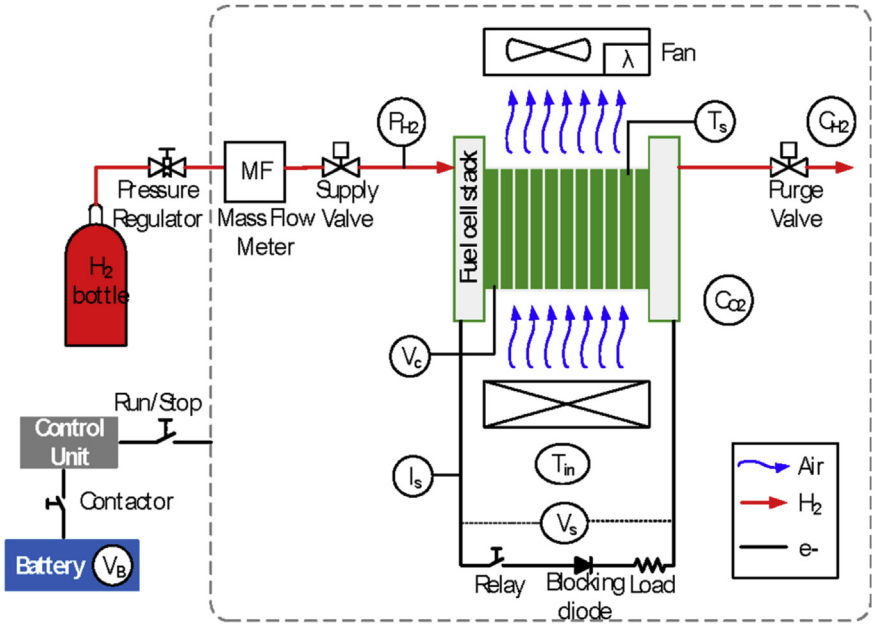


a) AC-PEFC diagram (stack + BoP).

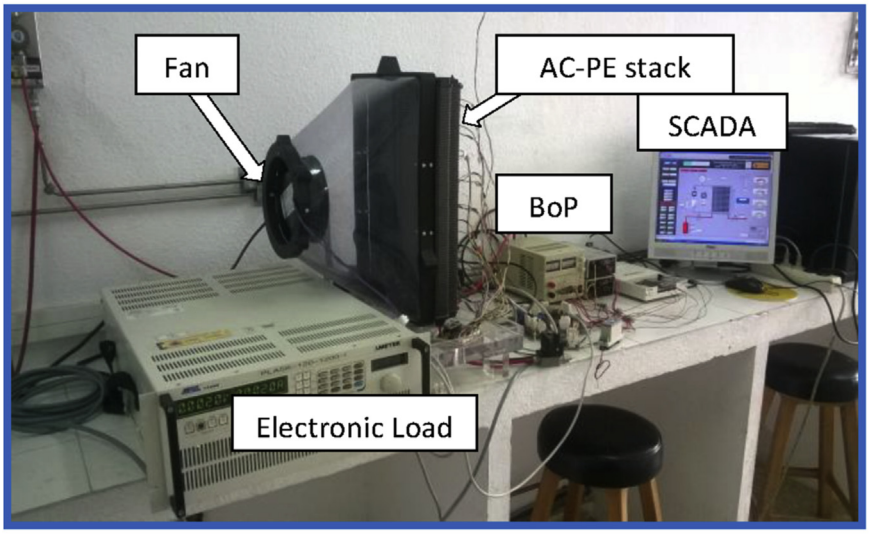


b) AC-PEFC real implementation (stack + BoP).

**Fig. 4 – Diagram and real implementation of the AC-PEFC under study.**

consumption, a supply valve to control the hydrogen entry and a hydrogen pressure sensor ($P_{H2}$) to measure the inlet anode pressure, complete the hydrogen input line. In the hydrogen outlet, a purge valve evacuates inert gases.

Then, once the AC-PEFC (stack + BoP) has been introduced, the first step is to characterize it. For this purpose the FCTESTNET/FCTESQA PEFC power stack performance testing procedure has been followed [33]. We can see (see Fig. 5) that the maximum stack power achieves 3 kW when the load current rises up to 75 A, while the stack voltage drops to 40 V (0.5 V for every cell, total 80, the limit specified by the manufacturer's recommendations). Moreover, the hysteresis phenomenon over the polarization curve (different upward and downward paths) can be easily distinguished [34]. Regarding hydrogen consumption, Fig. 6 compares the real hydrogen flow consumed with the hydrogen flow required for a proper operation according to manufacturer's data. It deserves to point out that in basis on real measures taken with the mass flow meter (see Fig. 4a), the real hydrogen flow rate follows a polynomial curve depending on load current according to (1):

$$Flow_{Hydrogen}(slpm) = 0.645 \cdot I_s - 0.00038 \cdot {I_s}^2 \quad (1)$$

where $I_s$ is the stack current which coincides with the load current.

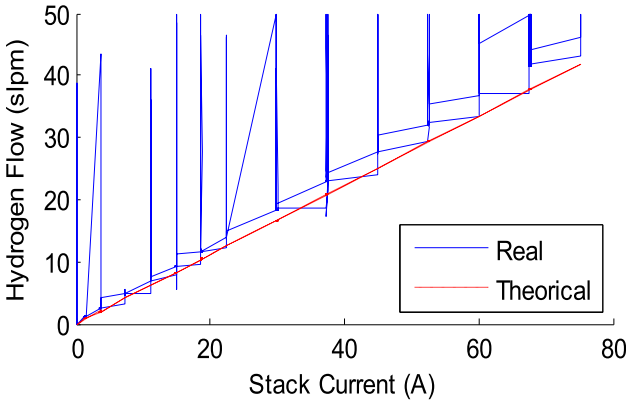


**Fig. 6 – Hydrogen flow consumption: measured value versus value provided by manufacturer.**

## BoP configurations study. Proposals for the fuel subsystem

Now, after the AC-PEFC characterization different BoP configurations will be studied and analysed in basis on the AC-PEFC response. This study consists on acting over different devices which integrate the hydrogen line (mass flow meter and hydrogen pressure sensor in the fuel inlet line and purge valve in the fuel outlet line). The way to have influence over the AC-PEFC will be placing a proportional control valve around the above-mentioned devices.

Then, the first two proposals for the BoP configuration are based on locating the proportional control valve downstream and upstream the mass flow meter (Fig. 7). This proportional control valve will allow controlling the hydrogen flow taking into account (1).

The first test will lie in adjusting the proportional control valve according to (2) which it is an empirical equation slightly below respect to real flow rate (1). The goal is to know if an AC-PEFC stack with DEA operation can work when the hydrogen flow input is limited, even if the flow restriction is very small compared to real flow.

$$Valve_{controlbelow}(slpm) = 0.63 \cdot I_s - 0.00033 \cdot {I_s}^2 \quad (2)$$

In the same way, the second test consists in adjusting the proportional control valve according to (3), a new empirical equation slightly above respect to real flow rate (1). In this case, we could compare the system performance when there is no restriction in the hydrogen flow input.

$$Valve_{controlabove}(slpm) = 0.65 \cdot I_s - 0.00038 \cdot {I_s}^2 \quad (3)$$

In the next two configurations, the proportional control valve is located downstream and upstream the hydrogen pressure sensor ($P_{H2}$) in the fuel inlet line (Fig. 8). In this case, the aim will not be to control the hydrogen flow but the hydrogen pressure. Then, we could draw some conclusions comparing the effects over the AC-PEFC performance when the hydrogen flow is controlled respect to the performance obtained when the control is applied over the hydrogen input.

Finally, the last two configurations consider the proportional control valve located downstream and upstream the hydrogen pressure sensor ($P_{H2}$), but in this case in the fuel outlet line (Fig. 9).

Then, with the proposed six configurations for the Fuel subsystem in an AC-PEFC, we could know what configuration favours a better system performance and how the control over some variables like hydrogen flow, inlet hydrogen pressure or

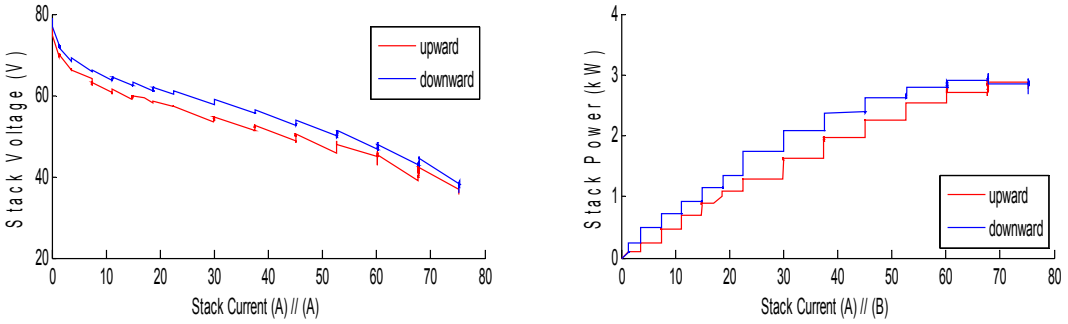


**Fig. 5 – Polarization and power curves. A: stack voltage (V) vs stack current (A). B: stack power (kW) vs stack current (A).**

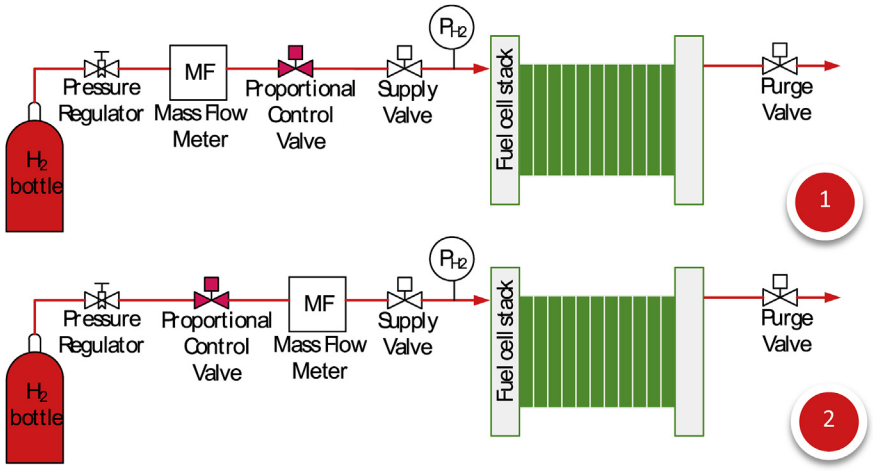


**Fig. 7 – Configurations 1 and 2: Proportional control valve downstream and upstream the mass flow meter.**

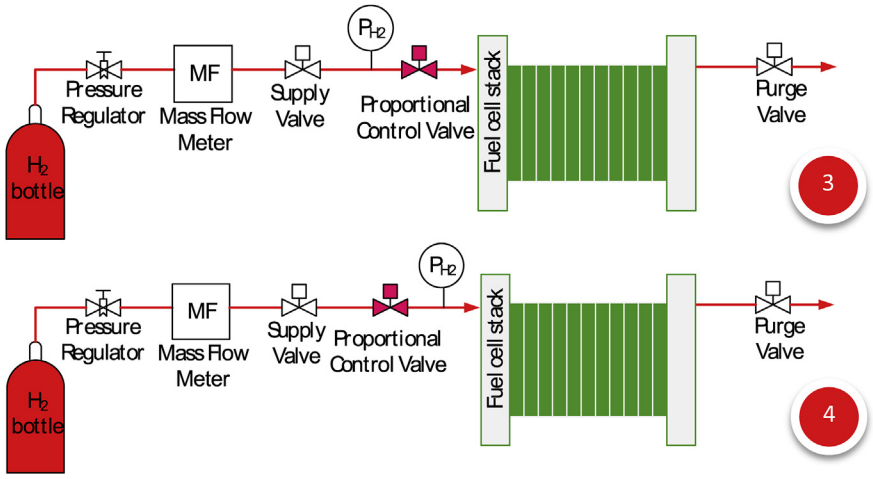


**Fig. 8 – Configurations 3 and 4: Proportional control valve downstream and upstream the hydrogen pressure sensor over the fuel inlet line.**

outlet hydrogen pressure can affect this performance when it comes to DEA operation.

## Experimental results

Once the different configurations have been presented, they have been implemented on the test bench shown in Fig. 4. Next, experimental results obtained from each configuration will be revealed.

### *Configurations 1 and 2: Proportional control valve downstream and upstream the mass flow meter*

In this case, the role of the proportional control valve is to establish the hydrogen input flow rate. As it has been previously commented, firstly the control valve will be placed downstream the mas flow and adjusted in the way that the hydrogen flow rate is slightly below (2) the real hydrogen flow rate (1). In this case, experimental results (Fig. 10) show that the restriction in the hydrogen input flow provokes the stack cannot provide the demanded power dropping it to zero. Notice that this restriction causes hydrogen starvation generating continuous airbags inside the fuel line and consequently leaks of hydrogen pressure. Regarding the cell structure shown in Fig. 1, in both sides of the MEA (anode and cathode), the air acts as reducing and oxidant agent, so no reaction takes place in the cell.

By against, keeping the proportional control valve downstream the mass flow meter but adjusted to allow passing more hydrogen than the real flow rate (3), experimental results (Fig. 11) show that proportional control valve is invisible in this configuration. That is, the hydrogen flow rate follows the load profile; the hydrogen pressure is keeping next to established value. Peaks on hydrogen pressure and flow coincide with hydrogen purges and air is supplied gradually more and more at time that the load current rises. Remember that the air must oxygenates and cools the stack when this is warming due to current increase. Then, we can conclude that in this configuration, proportional control valve can be

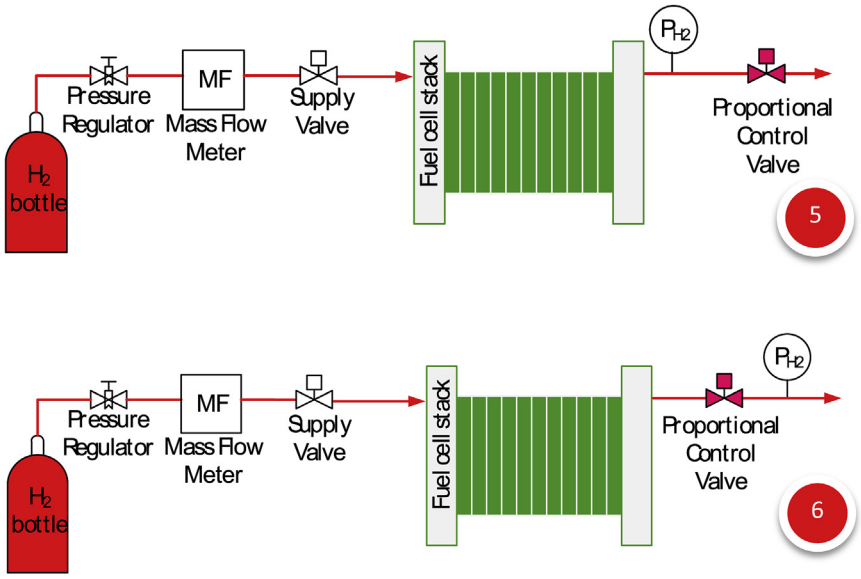


**Fig. 9 – Configurations 5 and 6: Proportional control valve downstream and upstream the hydrogen pressure sensor over the fuel outlet line.**

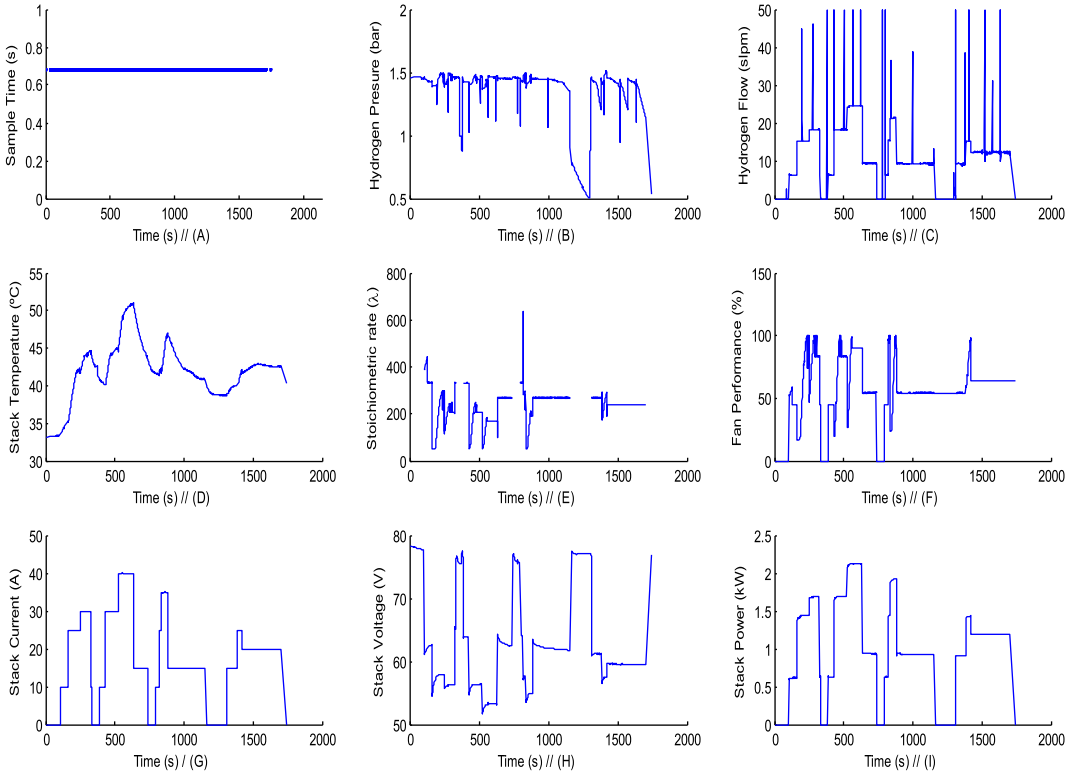


**Fig. 10 – AC-PEFC performance when the proportional control valve is placed downstream the mass flow meter and adjusted slightly below. From left to right and from top to bottom: (A)-Sample Time (s), (B)-Hydrogen Pressure (bar), (C)-Hydrogen Flow (slpm), (D)-Stack Temperature (°C), (E)-Air Stoichiometric Rate (λ), (F)-Fan Performance (%), (G)-Stack Current (A), (H)-Stack Voltage (V) and (I)-Stack Power (kW).**

removed from de BoP design because does not have any influence respect to system performance obtained from the original configuration shown in Fig. 4a.

Next, the proportional control valve is placed upstream the mass flow meter, and again adjusted slightly below (Fig. 12) and above (Fig. 13) the real hydrogen flow rate. When the proportional control valve is adjusted to control the input hydrogen flow slightly below, again the system stops working because of the hydrogen lack in the inlet line (Fig. 12), the hydrogen flow drops to zero and consequently the hydrogen

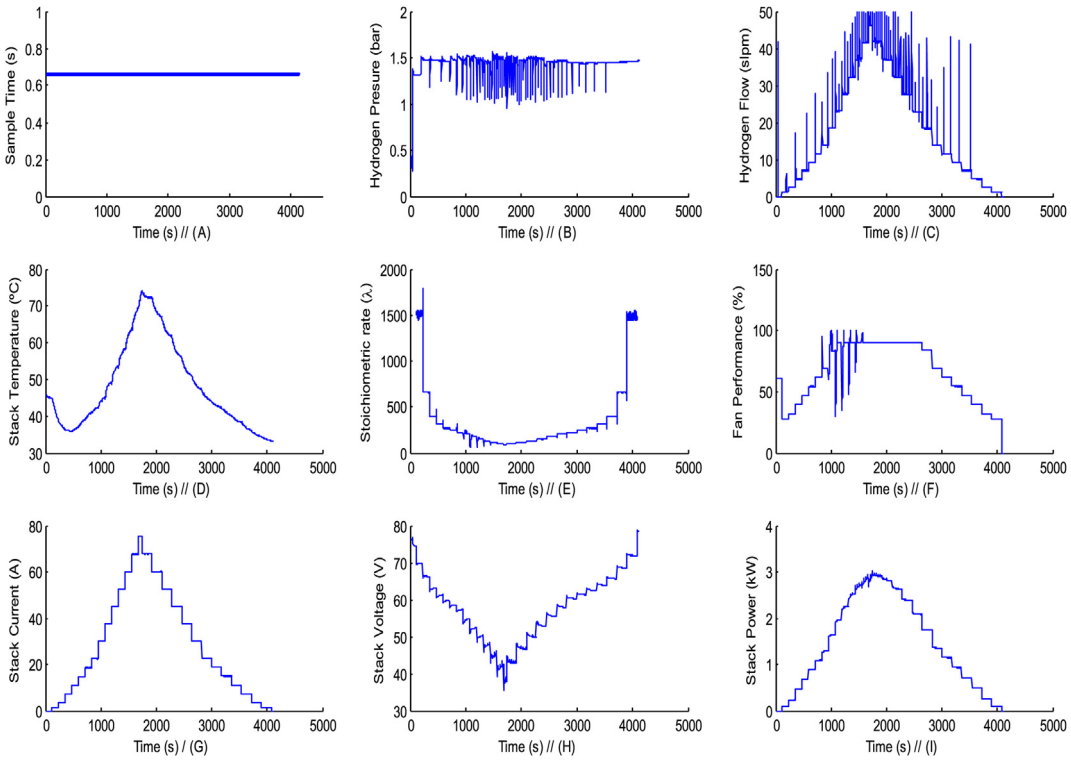


**Fig. 11 – AC-PEFC performance when the proportional control valve is placed downstream the mass flow meter and adjusted slightly above. From left to right and from top to bottom: (A)-Sample Time (s), (B)-Hydrogen Pressure (bar), (C)-Hydrogen Flow (slpm), (D)-Stack Temperature (°C), (E)-Air Stoichiometric Rate (λ), (F)-Fan Performance (%), (G)-Stack Current (A), (H)-Stack Voltage (V) and (I)-Stack Power (kW).**

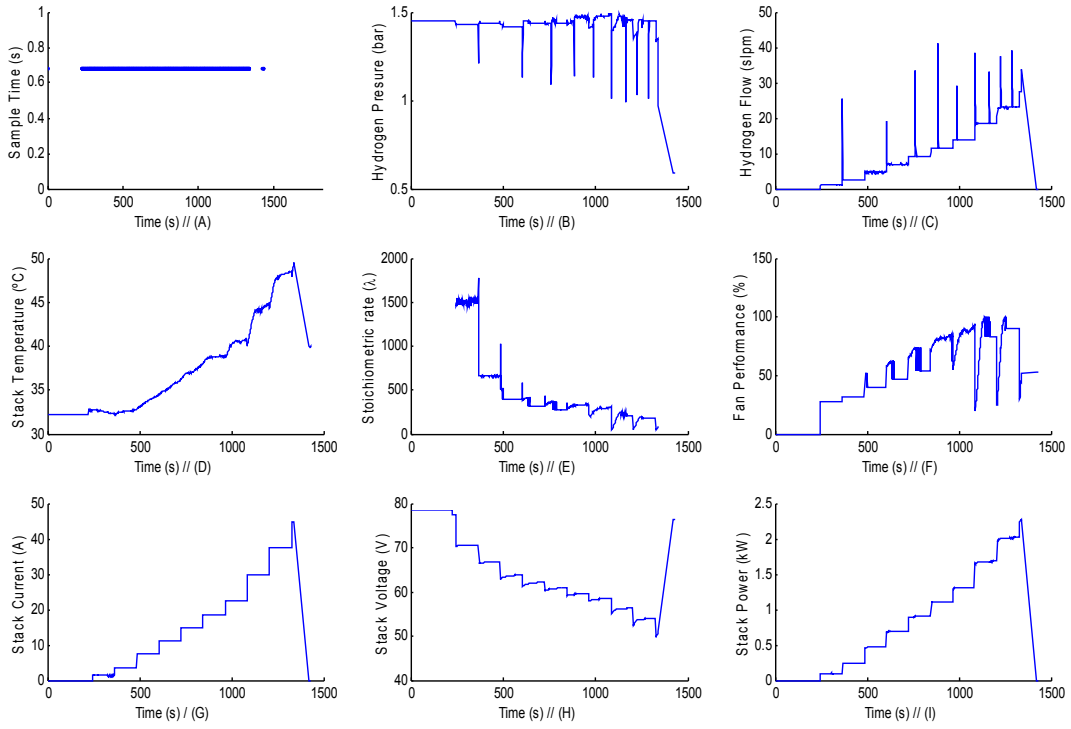


**Fig. 12 – AC-PEFC system performance when the proportional control valve is placed upstream the mass flow meter and adjusted slightly below. From left to right and from top to bottom: (A)-Sample Time (s), (B)-Hydrogen Pressure (bar), (C)-Hydrogen Flow (slpm), (D)-Stack Temperature (°C), (E)-Air Stoichiometric Rate (λ), (F)-Fan Performance (%), (G)-Stack Current (A), (H)-Stack Voltage (V) and (I)-Stack Power (kW).**

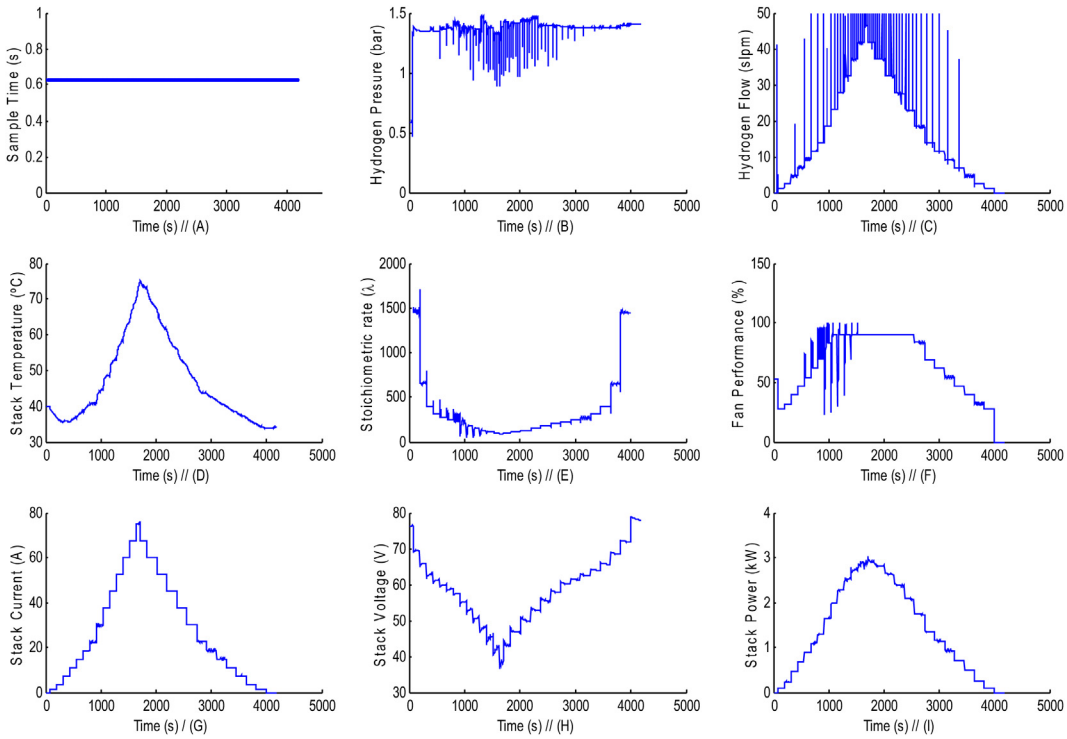


**Fig. 13 – AC-PEFC system performance when the proportional control valve is placed upstream the mass flow meter and adjusted slightly above. From left to right and from top to bottom: (A)-Sample Time (s), (B)-Hydrogen Pressure (bar), (C)-Hydrogen Flow (slpm), (D)-Stack Temperature (°C), (E)-Air Stoichiometric Rate (λ), (F)-Fan Performance (%), (G)-Stack Current (A), (H)-Stack Voltage (V) and (I)-Stack Power (kW).**

pressure, stack current and power as well. If the control valve is adjusted according to (3), experimental results are similar to that obtained in Fig. 11, when the valve was placed downstream the mass flow meter.

### *Configurations 3 and 4: Proportional control valve downstream and upstream the pressure sensor in the fuel inlet line*

Putting the proportional control valve around the pressure sensor in the fuel inlet line, the goal is to control the hydrogen input pressure. When the control valve is located downstream the pressure sensor, the scheme (Fig. 8-Configuration 3) looks like the feed-forward structure. Then, the control valve tries to anticipate to perturbations in the measure. This is what precisely happens during the first load steps (Fig. 14); along the way up of the load current, as consequence of the first load step, the hydrogen flow must increase. The stack consumes more hydrogen so the hydrogen pressure falls lightly (at $t = 50$ s), and the control valve tends to be completely closed to soften the pressure drop. Then, during the following load step, as current rises again the control valve continues closed in order to accumulate hydrogen in the fuel inlet line and achieve the established pressure value. This situation is responsible for the AC-PEFC shutdown; control valve closed, hydrogen doesn't enter in the anode and no reaction happens in the fuel cell.

In the second case, experimental results show effectively the pressure average value is fixed along the length of the test (Fig. 15). But it can be observed hydrogen pressure path is far to be stable, it presents continuous peaks even more frequent and deeper than in previous configurations. This is due to inter-relation between the hydrogen purge, pressure sensor and control valve. Hydrogen purge rate is fixed at 2300 A s (manufacturer's recommendation), and during the purge the hydrogen escapes freely; so the pressure drops with the purge. Then, the pressure sensor located just above (but in the inlet line) detects the pressure drop and consequently the control valve must act to correct the deviation. The control valve action affects over the hydrogen pressure which responds with an overshoot, and just next, another purge causing another hydrogen drop. These continuous undershoots and overshoots can be observed in Fig. 15B. What is common in those suitable configurations shown up to now (Figs. 11, 13 and 15) is the hydrogen pressure peaks are more frequent in the middle of the test (around $t = 2000$ s). Obviously, according to purge rate, higher current values means purges more frequent.

### *Configurations 5 and 6: Proportional control valve downstream and upstream the pressure sensor in the fuel outlet line*

Putting the proportional control valve around the pressure sensor in the fuel outlet line, the goal is to control the hydrogen pressure along the whole anode (from the input to the output). The first of these configurations locates the proportional control valve downstream the hydrogen pressure sensor in the fuel outlet line. This configuration shows that

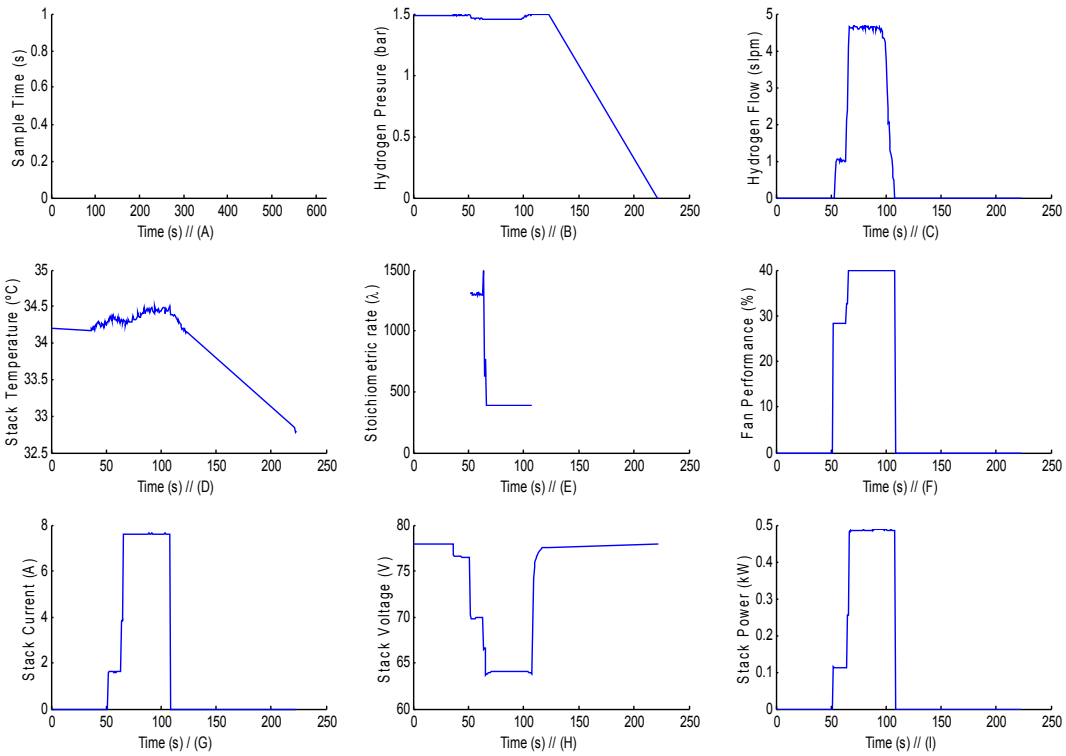


**Fig. 14 – AC-PEFC system performance when the proportional control valve is placed downstream the pressure sensor in the fuel inlet line. From left to right and from top to bottom: (A)-Sample Time (s), (B)-Hydrogen Pressure (bar), (C)-Hydrogen Flow (slpm), (D)-Stack Temperature (°C), (E)-Air Stoichiometric Rate (λ), (F)-Fan Performance (%), (G)-Stack Current (A), (H)-Stack Voltage (V) and (I)-Stack Power (kW).**

the PEFC system performance (Fig. 16) is similar to that obtained from Configuration 3 (Fig. 12). Again, the control valve tries to anticipate perturbations in the measure. As consequence of the increase in the load demand, the hydrogen flow must increase. The stack consumes more hydrogen, the hydrogen pressure falls and the control valve tends to be completely closed to soften the pressure drop.

However, when the proportional control valve is placed upstream the hydrogen pressure sensor in the fuel outlet line, experimental studies (Fig. 17) show that the goal is achieved: to maintain the hydrogen pressure along the whole fuel line fixed at the established value. Even more, in this case stack doesn't suffer continuous hydrogen pressure undershoots and overshoots as it happened in previous configurations. This is because now control valve acts like purge valve, but it purges hydrogen only when the hydrogen pressure begins to be deviated from the fixed value. That is hydrogen purge rate does not follow manufacturer's recommendations (2300 A s), but it depends on pressure variations. The risk of this apparent "good" configuration is that the purge rate is independent of the relation current–time. This implies inert gases are not removed properly from the anode side, leading in the long term to damage the membrane of the cells which integrate the PE stack.

Another issue which also requires attention is the hydrogen flow. As it can be observed in Fig. 17, in this case, hydrogen flow does not follow the load profile but it directly rises up to almost the maximum flow (40 slpm, see Fig. 6). As it can be observed in Fig. 17, initial pressure value is above the reference (1.48 bar vs 1.36 bar), so the control valve opens up to reduce the real value. This means to waste hydrogen, increasing the inlet flow. After that, hydrogen flow increases a little up to the highest value to allow the stack to supply the nominal power.

Finally, before moving onto the next section we would like to comment some aspects about the Oxidant/Cooling subsystem performance. As it has been commented in Section II, the main device of this subsystem is a speed adjustable fan which is responsible for providing enough air to oxygenate and cool the stack. From experimental results (Figs. 11, 13, 15 and 17), we can observe that in those viable configurations (Configuration 1, 2, 4 and 6) fan performance (speed percentage) raises at time that load current is going up to, in order to provide the air required for the stack reaction and to maintain the increasing stack temperature inside the range recommended by the manufacturer. When the fan performance is close to the maximum and the load current continues raising, the air stoichiometric rate (required air flow/total air flow) remains above the minimum recommended ($\lambda > 20$). Due to high stack temperature achieved at highest current values, the fan performance is kept at maximum even when the load current starts to drop; quick cooling process to maintain the stack temperature inside the recommended range at time that current falls.

When the stack temperature descends enough, it is not necessary to let the fan working at maximum so the fan speed is going to be reduced gradually. In the last configuration (Fig. 17), fan performance shape is slightly different to the rest;

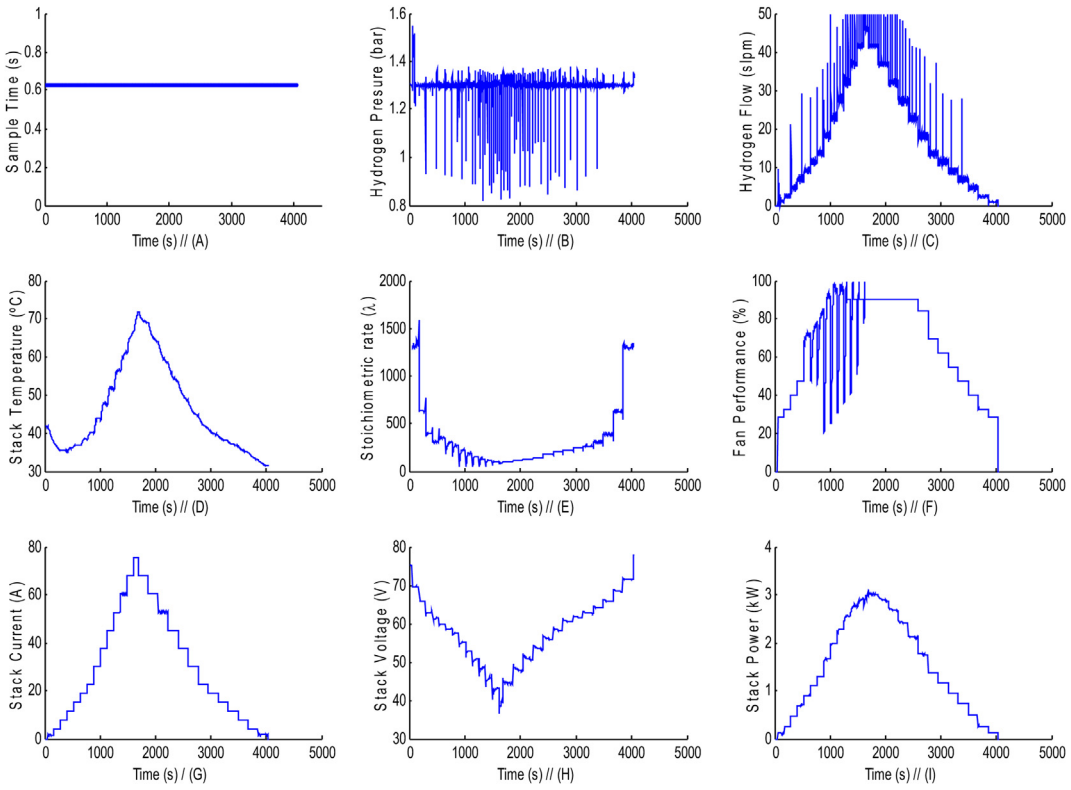


**Fig. 15 – AC-PEFC system performance when the proportional control valve is placed upstream the pressure sensor in the fuel inlet line. From left to right and from top to bottom: (A)-Sample Time (s), (B)-Hydrogen Pressure (bar), (C)-Hydrogen Flow (slpm), (D)-Stack Temperature (°C), (E)-Air Stoichiometric Rate (λ), (F)-Fan Performance (%), (G)-Stack Current (A), (H)-Stack Voltage (V) and (I)-Stack Power (kW).**

it does not follow the load profile. This is due precisely to load profile; in this last case maximum current value is achieved after t = 200 s, later than in previous tests. Then, before t = 200 s if load current is not too high and stack temperature is inside the range, fan does not need to be accelerate to avoid cells flooding.

## Discussion

In this paper, a half-dozen of possible configurations are proposed for the Fuel subsystem in an AC-PEFC. The diagram of the Fuel subsystem includes three basic devices: a mass flow meter, a pressure sensor and a purge valve. The different configurations are obtained adding a proportional control valve locating it downstream and upstream these basic devices. All the possible configurations have been implemented over the test bench shown in Fig. 4. Experimental results show that not all configurations are suitable and not all suitable configurations show identical AC-PEFC performance.

Among configurations no suitable, we can include those where the control valve is located around the mass flow meter and it is adjusted with a mass flow equation slightly below the measured real value, both downstream and upstream (Figs. 10 and 12). This conclusion corroborates one of the hypothesis suggested at the beginning of the paper, in Section I: the hydrogen mass flow control is not suitable for the DEA operation.

Moreover, configurations no suitable are also these where the control valve is placed downstream the hydrogen sensor both in the inlet and outlet fuel line (Configurations 3 and 5). This allow us to elucidate that configurations where the set sensor + actuator keeps the feed-forward structure do not guarantee neither pressure control nor proper stack performance.

By contrast, within the group of suitable configurations we can include all those which do not imply restrictions in the hydrogen mass flow, and all these where the hydrogen pressure is controlled with the set actuator + sensor (similar to a feed-back structure), configurations 1, 2, 4 and 6. Among these last configurations, hydrogen flow differs from one to another. This depends on the way to realise the pressure control and hydrogen purge. When the hydrogen pressure is controlled in the fuel inlet line and the purge rate is adjusted following the manufacturer's recommendations, the hydrogen consumption is optimised and we can observe how the hydrogen flow profile seems the load current profile (Figs. 11, 13 and 15). By contrast, when the hydrogen pressure is controlled in the fuel outlet line and the hydrogen purge depends on the pressure deviations, the hydrogen flow rises (Fig. 17), reducing the AC-PEFC efficiency (considering efficiency as the ratio between the electrical energy provided by the stack and the hydrogen supplied to stack).

Finally, these last configurations also differs in the way the hydrogen pressure responds along the time. In case the hydrogen pressure is controlled in the fuel inlet line, the

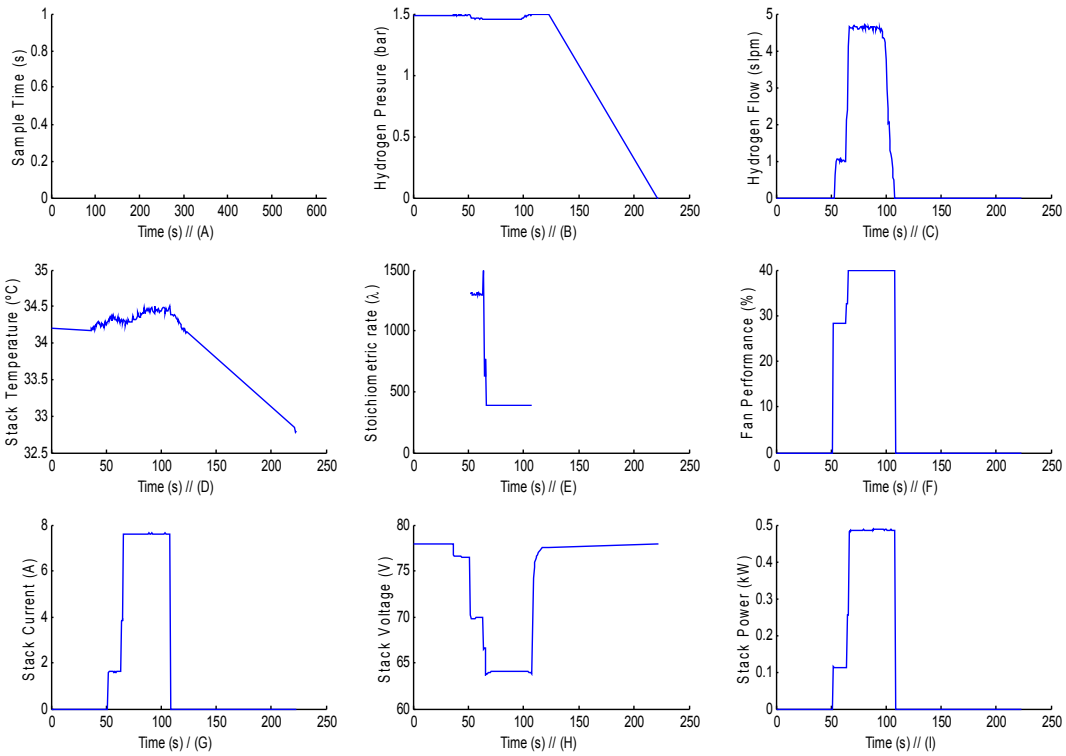


**Fig. 16 – AC-PEFC system performance when the proportional control valve is placed downstream the pressure sensor in the fuel outlet line. From left to right and from top to bottom: (A)-Sample Time (s), (B)-Hydrogen Pressure (bar), (C)-Hydrogen Flow (slpm), (D)-Stack Temperature (°C), (E)-Air Stoichiometric Rate (λ), (F)-Fan Performance (%), (G)-Stack Current (A), (H)-Stack Voltage (V) and (I)-Stack Power (kW).**

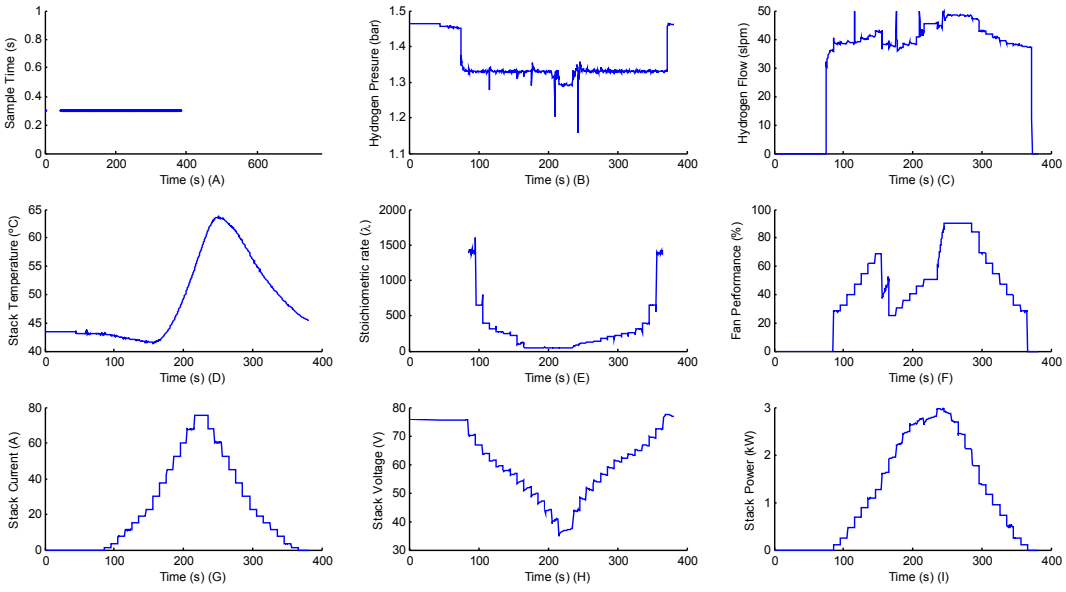


**Fig. 17 – AC-PEFC system performance when the proportional control valve is placed upstream the pressure sensor in the fuel outlet line. From left to right and from top to bottom: (A)-Sample Time (s), (B)-Hydrogen Pressure (bar), (C)-Hydrogen Flow (slpm), (D)-Stack Temperature (°C), (E)-Air Stoichiometric Rate (λ), (F)-Fan Performance (%), (G)-Stack Current (A), (H)-Stack Voltage (V) and (I)-Stack Power (kW).**

hydrogen purge follows the established rate; the pressure suffers continuous peaks derived from the purge rate and the action of the control valve. But in case the hydrogen pressure is controlled in the fuel outlet line, the hydrogen pressure evolution is a flat line, excepting some peaks derived from the pressure drops due to high power demand.

Table 1 summarises the main characteristics of the configurations analysed in this paper regarding aspects like

**Table 1 – Summary of analysed configurations.**

| # Configuration | Structure | Variable to control | Suitable | Stable Hydrogen pressure | Reduced Hydrogen consumption | Inert Gases Removed | Efficiency |
|---|---|---|---|---|---|---|---|
| 1a | Control valve downstream the mass flow 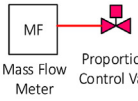  | $\dot{M}_{H2}$ | ✗ | | | | |
| 1b | Control valve downstream the mass flow meter, adjusted slightly above 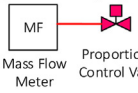  | $\dot{M}_{H2}$ | ✓ | ✗ | ✓ | ✓ | ✓ |
| 2a | Control valve upstream the mass flow meter, adjusted slightly below 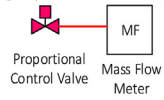  | $\dot{M}_{H2}$ | ✗ | | | | |
| 2b | Control valve upstream the mass flow meter, adjusted slightly above 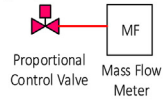  | $\dot{M}_{H2}$ | ✓ | ✗ | ✓ | ✓ | ✓ |
| 3 | Control valve downstream the pressure sensor in the fuel inlet line 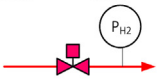  | $P_{H2}$ | ✗ | | | | |
| 4 | Control valve upstream the pressure sensor in the fuel inlet line 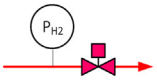  | $P_{H2}$ | ✓ | ✗ | ✓ | ✓ | ✓ |
| 5 | Control valve downstream the pressure sensor in the fuel outlet line 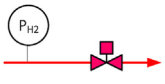  | $P_{H2}$ | ✗ | | | | |
| 6 | Control valve upstream the pressure sensor in the fuel outlet line 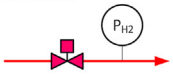  | $P_{H2}$ | ✓ | ✓ | ✗ | ✗ | ✗ |

ability to maintain stable the hydrogen pressure, hydrogen consumption, possibility to remove inert gases as frequent as manufacturer recommends, AC-PEFC efficiency (refereeing provided electrical power respect to hydrogen consumption) and definitely the suitability of the proposed configurations.

## Conclusions

This paper presents a comprehensive experimental analysis of six possible configurations of the Fuel subsystem in an AC-PEFC. It has been justified that studies in which the Fuel subsystem is investigated are hard to find on the scientific literature. It seems like the Fuel subsystem configuration would not have influence over the whole system performance. Contrary to what one might think, and in basis on experimental results, this paper has shown how the AC-PEFC performance is conditioned by the Fuel subsystem configuration.

To carry out the study, the AC-PEFC has been previously characterised in a test bench developed by authors.

After that, different Fuel subsystem configurations have been analysed in basis on the AC-PEFC response.

Regarding experimental results, we can assert that Fuel subsystem configurations where the hydrogen mass flow is restricted, even if the mass flow rate is slightly below the real mass flow, are not suitable.

Within the group of suitable configurations are those that do not involve restrictions in the hydrogen mass flow, and all these where the hydrogen pressure is controlled with the set actuator + sensor (feed-back structure).

Moreover, within these last configurations, hydrogen flow response depends on the way to realise the pressure control and hydrogen purge. When the hydrogen pressure is controlled in the fuel inlet line, the purge rate can follows the manufacturer's recommendations and the hydrogen consumption is optimised seeming the load current profile. In case the hydrogen pressure is controlled in the fuel outlet line, the hydrogen purge only happens when there are deviations in the pressure measure. And this causes the hydrogen flow rises.

As conclusion we can say that in an AC-PEFC with DEA operation mode there is not a specific configuration of the Fuel subsystem which could be called the “best configuration”. As it has been demonstrated, each configuration has its own advantages. Then for example, if we expect to have a precise control of the pressure in the hydrogen line, the best option is to control the hydrogen pressure in the outlet line and hydrogen will be only purged when pressure measure varies from the reference value. However, if we want to obey manufacturer's recommendations in relation to purge rate (guaranteeing the inert gases removing), and optimise the hydrogen flow consumption, hydrogen pressure will suffer continues peaks derived from the periodic purges.

Finally, main characteristics of analysed configurations have been summarised in Table 1, making easier to compare them for an overview before to implement the BoP of an AC-PEFC.

## REFERENCES


[1] Mehta V, Cooper JS. Review and analysis of PEM fuel cell design and manufacturing. J Power Sources 2003;114:32–53.

[2] Sammes N. Fuel cell technology: reaching towards commercialization. Springer Sci Bus Media 2006. ISBN 13: 978-1-85233-974-6.

[3] Faghri BSM. Transport phenomena in fuel cells, vol. 19. WIT Press; 2005.

[4] Siegel C. Review of computational heat and mass transfer modeling in polymer-electrolyte-membrane (PEM) fuel cells. Energy 2008;33:1331–52.

[5] Varigonda S, Kamat M. Control of stationary and transportation fuel cell systems: progress and opportunities. Comput Chem Eng Sep. 2006;30(10–12):1735–48.

[6] Vasallo MJ, Bravo JM, Andújar JM. Optimal sizing for UPS systems based on batteries and/or fuel cell. Appl Energy 2013;105:170–81.

[7] Segura F, Durán E, Andújar JM. Design, building and testing of a stand alone fuel cell hybrid system. J Power Sources 2009;193:276–84.

[8] Özgirgin E, Devrim Y, Albostan A. Modeling and simulation of a hybrid photovoltaic (PV) module-electrolyzer-PEM fuel cell system for micro-cogeneration applications. Int J Hydrogen Energy October 2015;40:15336–42.

[9] Nguyen HQ, Aris AM, Shabani B. PEM fuel cell heat recovery for preheating inlet air in standalone solar-hydrogen systems for telecommunication applications: an exergy analysis. Int J Hydrogen Energy October 2016;41:2987–3003.

[10] Lui JX, Laghrouche S, Ahmed F-S, Wack M. PEM fuel cell air-feed system observer design for automotive applications: an adaptive numerical differentiation approach. Int J Hydrogen Energy 2014;39(30):17210–21.

[11] Zhang J, Xie Z, Zhang J, Tang Y, Song C, Navessin T, et al. High temperature PEM fuel cells. J Power Sources 2006;160:872–91.

[12] Zhang G, Kandlikar SG. A critical review of cooling techniques in proton exchange membrane fuel cell stacks. Int J Hydrogen Energy 2012;37(3):2412–29.

[13] Wang Y-X, Xuan D-J, Kim Y-B. Design and experimental implementation of time delay control for air supply in a polymer electrolyte membrane fuel cell system. Int J Hydrogen Energy Oct. 2013;38(30):13381–92.

[14] Cordner M, Matian M, Offer GJ, Hanten T, Spofforth-Jones E, Tippetts S, et al. Designing, building, testing and racing a low-cost fuel cell range extender for a motorsport application. J Power Sources 2010;195(23):7838–48.

[15] Ahn JW, Choe SY. Coolant controls of a PEM fuel cell system. J Power Sources 2008;179:252–64.

[16] Han HS, Cho C, Kim SY, Hyun JM. Performance evaluation of a polymer electrolyte membrane fuel cell system for powering portable freezer. Appl Energy 2013;105:125–37.

[17] Segura F, Andújar JM. Step by step development of a real fuel cell system. Design, implementation, control and monitoring. Int J Hydrogen Energy 2015;40(15):5496–508.

[18] Philipps F, Simons G, Schiefer K. Dynamic investigation of PEFC stacks in interaction with the air supply system. J Power Sources Mar. 2006;154(2):412–9.

[19] Kim Y-B. Improving dynamic performance of proton-exchange membrane fuel cell system using time delay control. J Power Sources 2010;195(19):6329–41.

[20] Himanen O, Hottinen T, Tuurala S. Operation of a planar free-breathing PEMFC in a dead-end mode. Electrochem Commun 2007;9:891–4.

[21] Eckl R, Zehtner W, Leu C, Wagner U. Experimental analysis of water management in a self-humidifying polymer electrolyte fuel cell stack. J Power Sources 2004;138:137–44.
[22] del Real AJ, Arce A, Bordons C. Development and experimental validation of a PEM fuel cell dynamic model. J Power Sources 2007;173:310–24.
[23] Hwang JJ, Zou ML. Development of a proton exchange membrane fuel cell cogeneration system. J Power Sources 2010;195:2579–85.
[24] Gerbec M, Jovan V, Petrovčič J. Operational and safety analyses of a commercial PEMFC system. Int J Hydrogen Energy 2008;33:4147–60.
[25] Soupremanien U, Le Person S, Favre-Marinet M, Bultel Y. Tools for designing the cooling system of a proton exchange membrane fuel cell. Appl Therm Eng 2012;40:161–73.
[26] Marcinkoski J, James BD, Kalinoski JA, Podolski W, Benjamin T, Kopasz J. Manufacturing process assumptions used in fuel cell system cost analyses. J Power Sources 2011;196(12):5282–92.
[27] Na Y, Suh J, Song I, Choi K-H, Choi H, Kim KB, Park J-Y. Stable operation of air-blowing direct methanol fuel cell stacks through uniform oxidant supply by varying fluid flow fixtures and developing the flow sensor. Int J Hydrogen Energy 2011;36(15):9205–15.
[28] Kim BJ, Kim MS. Studies on the cathode humidification by exhaust gas recirculation for PEM fuel cell. Int J Hydrogen Energy 2012;37(5):4290–9.
[29] Hinaje M, Rael S, Caron JP, Davat B. An innovating application of PEM fuel cell: current source controlled by hydrogen supply. Int J Hydrogen Energy 2012;37(17):12481–8.
[30] Rodatz P, Tsukada A, Mladek M, Guzzella L. Efficiency improvements by pulsed hydrogen supply in PEM fuel cell systems. World Congr 2002;15(1):1509.
[31] Chen J, Siegel JB, Stefanopoulou AG, Waldecker JR. Optimization of purge cycle for dead-ended anode fuel cell operation. Int J Hydrogen Energy Apr. 2013;38(12):5092–105.
[32] Fuel cell stack product manual and integration guide. 2011.
[33] Antoni L. FCTESTNET/FCTESQA PEFC power stack performance testing procedure I. Polarisation curve test method. 2009.
[34] Hou J. A study on polarization hysteresis in PEM fuel cells by galvanostatic step sweep. Int J Hydrogen Energy 2011;36(12):7199–206.